International Journal of Pharmacology

ISSN 1811-7775

science alert

ansinet
Asian Network for Scientific Information

OPEN ACCESS International Journal of Pharmacology

ISSN 1811-7775
DOI: 10.3923/ijp.2022.947.961

Research Article
Improving Cognitive Function Through Inhibiting the Activation of Microglia by Jia Wei Kai Xin San on Alzheimer's Disease Rats

[1]Yang Liu, [2]Shi-Yu Chen, [1]Jing-Jing Ma, [3]Yu-Qing Jiang, [2]Feng Gu and [2]Hong-Xin Zheng

[1]College of Traditional Chinese Medicine, Liaoning University of Traditional Chinese Medicine, Shenyang, 110032, People's Republic of China
[2]Graduate School, Liaoning University of Traditional Chinese Medicine, Shenyang 110032, People's Republic of China
[3]Teaching and Experiment Center, Liaoning University of Traditional Chinese Medicine, Shenyang 110032, People's Republic of China

Abstract

Background and Objective: Alzheimer's disease is a primary central degenerative disease, most of the current treatment drugs cannot delay or prevent the progression of the disease, only temporarily alleviating the symptoms. To investigate the mechanism of Jia Wei Kai Xin San on inhibiting the activation of microglia and realizing the anti-inflammatory effect by inhibiting the TLR4/MyD88/NF-κB signalling pathway in Alzheimer's disease rats. **Materials and Methods:** The rat model of AD was established by injecting $A\beta^{1-42}$ into the lateral ventricle of the rat. Then, the rats were treated with different concentrations of Jia Wei Kai Xin San decoction by oral gavage for 6 weeks and the cognitive function and exploratory behaviour of the rats were measured. The expression levels of inflammatory factors in serum, cortex and hippocampus of the rats were detected by ELISA and Western blot and the pathological changes of the cerebral cortex were observed by HE staining. The co-expression of microglia markers in brain tissue was detected by the immunofluorescence double-label method. **Results:** All doses of Jia Wei Kai Xin San could improve the cognitive function and exploration behaviour of rats, inhibit the content of inflammatory factors in serum, cortex and hippocampus, alleviate the pathological changes of the cerebral cortex, inhibit the differentiation of microglia to M1-type and promote the polarization to M2-type. **Conclusion:** Jia Wei Kai Xin San could improve the cognitive function of Alzheimer's disease rats by decreasing the levels of inflammatory factors in serum and brain tissue, inhibiting the over-activation of TLR4/MyD88/NF-κB pathway in brain tissue and promoting the polarization of microglia into M2 type.

Key words: Jia Wei Kai Xin San, Alzheimer's disease, Microglia, TLR4/MYD88/NF-κB, signalling pathway

Citation: Liu, Y., S.Y. Chen, J.J. Ma, Y.Q. Jiang, F. Gu and H.X. Zheng, 2022. Improving cognitive function through inhibiting the activation of microglia by Jia Wei Kai Xin San on Alzheimer's disease rats. Int. J. Pharmacol., 18: 947-961.

Corresponding Author: Feng Gu and Hong-Xin Zheng, College of Traditional Chinese Medicine, Liaoning University of Traditional Chinese Medicine, 79thChongshan East Road, Shenyang 110032, Liaoning, People's Republic of China

Competing Interest: The authors have declared that no competing interest exists.

Data Availability: All relevant data are within the paper and its supporting information files.

INTRODUCTION

Alzheimer's disease (AD) is a series of diseases that are related to age and specific neuropathology and ultimately lead to death by cognitive decline. As of 2019, nearly 5.8 M Americans had been diagnosed with AD. This number is expected to grow to 13.8 M by 2050[1]. The AD is characterized by memory impairment, aphasia, apraxia, agnosia, impaired visuospatial skills, executive dysfunction and personality and behavioural changes. Amyloid (Aβ) is one of the important biomarkers in the progression of AD. The conversion of microglia from M0-resting states to M1-activated states has been reported to be a key factor in mediating the development of an inflammatory response to AD[2,3]. However, M2 type microglia play an important role in clearing away Aβ deposition and inhibiting the occurrence of inflammatory reactions during the development of AD[4]. It has also been shown that Aβ deposition is an important factor that induces the activation of NF-κB signalling pathways and thus mediates the development of the inflammatory response[5,6].

Kaixin San (KS) was first written in *Qianjin Fang* by Sun Simiao in Tang Dynasty. The prescription is composed of ginseng, polygala, Tuckahoe and rhizome acorigraminei. It is now used in the treatment of diseases such as Alzheimer's disease and vascular dementia with memory dysfunction as the main manifestation[7-9]. It has been reported that the active ingredient in KS can interact with IL-1 and TNF-α inflammatory factors to inhibit inflammation and the development of inflammation throughout the whole pathogenic process of Alzheimer's disease[10], which shows that KS may have a therapeutic effect on the whole course of Alzheimer's disease. Ginseng saponins Rb2 have also been shown to reduce the damage of rat cortical neurons and protect them from microglial activation[11]. It can be seen that the treatment of KS for AD is mainly based on the regulating effect of KS on the activation of microglia, which inhibits the occurrence of inflammatory reactions.

Jiawei Kaixin San (JKS) has been the focus of our team for many years. Based on traditional KS, JKS is added with four traditional Chinese medicines including prepared rhizome of rehmannia, yam, Cornus Officinalis and prepared large head atractylodes rhizome and has been used to treat AD for many years. It has been found that JKS could improve the cognitive dysfunction of AD patients, but the mechanism was not clear. In this study, based on the literature support and the observation of the clinical efficacy of JKS, the mechanism of JKS on improving cognitive function and anti-inflammation in AD rats was expounded through animal experiments.

MATERIALS AND METHODS

Study area: This study was carried out at Liaoning University of Traditional Chinese Medicine, Shenyang, China from May, 2020 to July, 2021.

Animals: Sixty-two SPF-grade Sprague-Dawley rats, half male and half female (6-8 weeks old, weighing 200±20 g), were provided by Liaoning Changsheng Biotech Co., Ltd. (Certificate No.: No.211002300012541, Laboratory Animal Manufacturing License No.: SCXK (Liao) 2015-0001). After purchase, they were fed in the Laboratory Animal Centre of Liaoning University of Traditional Chinese Medicine. Laboratory ambient temperature was 23±2°C and the humidity was 50±5%, adaptive feeding for 1 week with free diet and drinking water.

Sixty-two rats were randomly divided into two groups: Sham-operated group (SO group, n = 13) and model group (n = 49). Then the AD rat model was replicated and the water maze test and open-field test were performed 1 week after the operation to evaluate the cognitive function of the rats. One rat was randomly selected from the SO group and model group, respectively and the brain was stained with HE to observe the pathological changes of the brain.

According to the evaluation results of the model, the rats were randomly divided into four groups: Model control group (MC group), high-dose group (HD group), medium-dose group (MD group) and low-dose group (LD group).

Chemical and reagents: The JKS was purchased from the Outpatient Pharmacy of the Affiliated Hospital of Liaoning University of Traditional Chinese Medicine. The total dosage of smart granules was 130 g and the clinical dosage was 14 g/dose. According to the equivalent dose conversion formula of humans and rats, the dosage of rats (g kg^{-1}) = dosage of humans (14 g kg^{-1}) × 6.3, the equivalent dosage of rats is about 1.3 g kg^{-1} b.wt., which is the dosage for MD group. The dosage for the HD group is 2.6 g kg^{-1} b.wt. and the dosage for the LD group is 0.65 g kg^{-1} b.wt.

The $A\beta^{1-42}$ (SCP0038-500 UG) was purchased by Sigma. The TNF-α, IL-1β, IL-6 and IFN-γ kits were purchased from Wuhan Youersheng Biotech Co., Ltd. The $A\beta^{1-42}$ antibody was purchased from Beijing Borson Biotechnology Co., Ltd. and the cat. No. is BS-0107R. Anti-TLR4 (ab13867), anti-MYD88 (ab219413), anti-NF-κB (ab16502), anti-p-NF-κB (ab239882), anti-CD86 (B7-2) (ab220188), anti-CD206 (ab64693) and anti-Iba-1 (ab283319) antibodies were purchased from

Abcam. Anti-CD80 (B7-1) (# 54521) and anti-Arg-1 (# 93668) antibodies were purchased from CST. Protein extraction kits and fluorescence labelling secondary antibodies were purchased from Biyuntian Biotechnology Research Institute. Protein markers are purchased from Thermo.

The $A\beta^{1-42}$, 100 μg in 100 μL of physiological saline in a 37 incubator, incubated for a week, during which the solution was shaken once a day to become aggregated and stored in a 4 refrigerator.

Model replication: The AD rat model was replicated by injection of $A\beta^{1-42}$ into the lateral ventricle. The rats were anaesthetized by intraperitoneal injection of 3% sodium pentobarbital (1.5 mL kg^{-1}). Then the rats were fixed on the rat brain stereotactic apparatus in the prone position. Reference was made to the rat brain stereotactic map[12]. Taking the rat brain fontanelle as the origin, the rat brain stereotactic apparatus was used to locate the origin of 4.0 mm backwards and 2.0 mm bilateral paracentesis of the midline. After labelling, the rats were drilled with the skull and the meninges were not cut. After that, a 3.0 mm vertical needle was used to inject $A\beta^{1-42}$ solution (1 μL/100 g b.wt.) into the lateral ventricles. The needle was left for 5 min, then the needle was withdrawn, the small hole of the skull was closed with bone wax and the skin was sutured. The model was evaluated for success after 2 weeks of normal feeding.

In the SO group, the rats were operated in the same way as above and an equal amount of normal saline was injected into the lateral ventricle.

Administration of JKS: The rats in the MC, HD, MD and LD group were administered by oral gavage with normal saline, high concentration of JKS (0.26 g mL^{-1}), the medium concentration of JKS (0.13 g mL^{-1}) and low concentration of JKS (0.065 g mL^{-1}), respectively and the dosage was 10 mL kg^{-1} b.wt., once a day for 6 weeks.

Water maze assay: A localization navigation experiment was used to assess the spatial learning capacity in rats. Each rat was swimming in water from three quadrants excluding the target quadrant, each day for a maximum of 120 sec. When the rat climbs the platform and stays for 5 sec or more within 120 sec, the test is regarded as finished and the time elapsed is recorded as the incubation period. If the rat does not find the platform within 120 sec, place the rat on the platform and stay for 10 sec to allow the rat to learn and adapt and record the latency as 120 sec.

A space exploration experiment was used to judge the spatial memory ability of the rats. The experiment environment and the water temperature and position navigation test remained the same, except that the platform under the water was removed and the rats were then placed in the pool from the northwest quadrant. The swimming path of the rats was recorded and analyzed within 120 sec and the remaining quadrants do not require testing. The number of rats crossing the original platform and the percentage of the total time in the target quadrant time was recorded.

Open-field assay: Place the rat in the centre of the open-field analysis box and record the number of dislodgement times of the forelimbs and the number of squares traversed in 5 min.

Aβ deposition level assay: The level of Aβ protein in the hippocampus was detected by Western blot. Fifty milligrams fresh hippocampus tissue was added with 450 μL protease inhibitor-containing lysate. The tissue homogenate was prepared by a high-speed homogenate mechanism. The tissue homogenate was lysed in the ice bath for 15 min and centrifuged at 12,000 g for 15 min. The supernatant was obtained as total protein. The BCA method is used to measure the protein concentration. Add 5× protein loading buffer in a 4:1 ratio, mix the solution fully, boil the solution for 5 min and denature the protein. Perform vertical electrophoresis according to the loading volume of 50 μg per well. Transfer the protein to the PVDF membrane by the wet transfer method. After membrane washing, seal the membrane with 5% BSA solution for 1 h. Incubate with the anti-$A\beta^{1-42}$ working solution (1:800) at 4°C overnight. Reheat the membrane at room temperature for 2 hrs the next day. Take out the PVDF membrane, wash the membrane with TBST buffer 6 times and 5 min per time. Then incubate the membrane with HRP-labeled goat anti-rabbit (1:2000) at room temperature for 2 hrs. Take out the PVDF membrane and wash the membrane with TBST buffer 6 times and 5 min per time. The PVDF membrane was placed in the gel image analysis system and the ECL luminescence fluid was added to collect the image.

Content of the inflammatory factor: The frozen left cerebral cortical tissue was collected and the protease inhibitor-containing lysate was added at the ratio of 900 μL per 100 mg of brain tissue. The tissue homogenate was prepared by the high-speed homogenate mechanism and then centrifuged at 3000 rpm for 10 min. The supernatant was collected to detect the content of inflammatory factors in the brain tissue.

The contents of TNF-α, IL-1β, IL-6 and IFN-γ in brain homogenate and serum were measured by ELISA kit. Follow the instructions in the kit accessories manual.

Levels of activation and polarization of microglia: The co-expression of Iba-1/CD80 (B7-1), Iba-1/CD86 (B7-2), Iba-1/CD206, Iba-1/Arg-1 and Iba-1/p-NF-κB in brain tissue was detected by immunofluorescence double labelling. After wax removal and hydration, antigen repair was performed using a thermal repair method (citrate buffer soaked the sections and heated in a boiling water bath for 20 min). The slides were then placed flat in a wet box, coated around the tissue circle with an immunohistochemistry pen, 0.1% TritonX-100 was added to the centre of the circle to destroy the membrane, staid at room temperature for 5 min and washed with PBS buffer 3 times for 5 min per time. After breaking the membrane, 5% BSA solution was added and blocked and incubated at 37 for 10 min. The primary antibody was diluted with a blocking solution. The Iba-1 was double-labelled with CD80 (B7-1), CD86 (B7-2), CD206, Arg-1 and p-NF-κB and incubated overnight at 4 in a refrigerator. Rewarm it at room temperature for 2 hrs the next day, wash it with PBS buffer 6 times for 5 min per time. Add FITC-labeled goat anti-rabbit antibody and PE-labeled goat anti-mouse antibody mixture, respectively. The solution was added to the slide and incubated at 37 for 2 hrs and washed with PBS buffer 6 times for 5 min per time. Cover the slide with a fluorescence-resistant quench DAPI. The number of positive cells in each field was counted and the same slide was counted in 5 fields.

Level of TLR4/MYD88/NF-κB signal pathway activation in the cerebral cortex: The expression levels of TLR4, MYD88, NF-κB and p-NF-κB in the cerebral cortex of rats were detected by the western-blot method, which was the same as the Aβ deposition level assay section.

Data analysis: The SPSS 22.0 software was used to analyze the experimental data and GraphPad Prism 5 software was used to perform the histograms and line charts.

RESULTS

Model evaluation: The results of water maze training, space exploration experiment and positioning navigation experiment after training of rats in each group are shown in Fig. 1. Positioning navigation heat maps of rats in the SO group in Fig. 1a and model group in Fig. 1b were measured and the time changes of water maze positioning navigation in Fig. 1c and the number of crossing platforms in Fig. 1d were counted. It showed that two groups of rats began to perform water maze exercises a week after the operation, for 5 days in a row and on the 6th day, the positioning navigation and space exploration experiments were performed. On the 1st to 5th day, the positioning time of the two groups of rats was shortened day by day and that of the SO group was faster than that of the model group. The results of the experiment on the 6th day showed that the positioning time of rats in the model group was significantly longer than that of the SO group ($p<0.01$) and the times of crossing the platform was significantly less than that of the SO group ($p<0.01$).

The experimental results of rats in each group after open field training and after training are shown in Fig. 2. Open-field test heat map of rats in SO group in Fig. 2a and open-field test heat map of rats in model group in Fig. 2b were measured and the number of body uprightness and the number of facial washing movements in the open field test of rats in Fig. 2c was counted. It showed that the number of erection and face washing movements in the model group were significantly decreased compared with the SO group ($p<0.05$).

The pathological photos of brain tissue of rats in the two groups are shown in Fig. 3. The cortex of rats in the SO group in Fig. 3a) and model group in Fig. 3b and the hippocampus of rats in the SO group in Fig. 3c and model group in Fig. 3d were all measured. It showed that in the SO group, the number of nerve cells in the cerebral cortex was large and the arrangement was dense. In the model group, the number of nerve cells in the cerebral cortex was small and the arrangement level was not regular. In the SO group, the hippocampal neurons were arranged in an orderly manner, with complete structure and round nuclei. In the model group, the neuron cell structure was incomplete, the arrangement was not tight and the number of cells decreased obviously.

Cognitive function of rats: The test results of the cognitive function of rats in each group are shown in Fig. 4. The time changes of water maze positioning navigation in Fig. 4a and the number of crossing platforms in Fig. 4b were counted. Figure 4b shows the space exploration experiment. The x-axis is each group and the y-axis is the number of times each group of rats crosses the quadrant where the platform is located. The positioning navigation heat map of rats in the SO group in Fig. 4c, MC group in Fig. 4d, HD group in Fig. 4e, MD group in Fig. 4f and LD group in Fig. 4g were measured. The results of the water maze test showed that the positioning time of rats in each group was shortened gradually by water maze practice and the escape latency of rats in the SO group was shortened the fastest. Compared with the SO group, the escape latency of the other groups was significantly increased ($p<0.01$) and the number of traversing platforms was

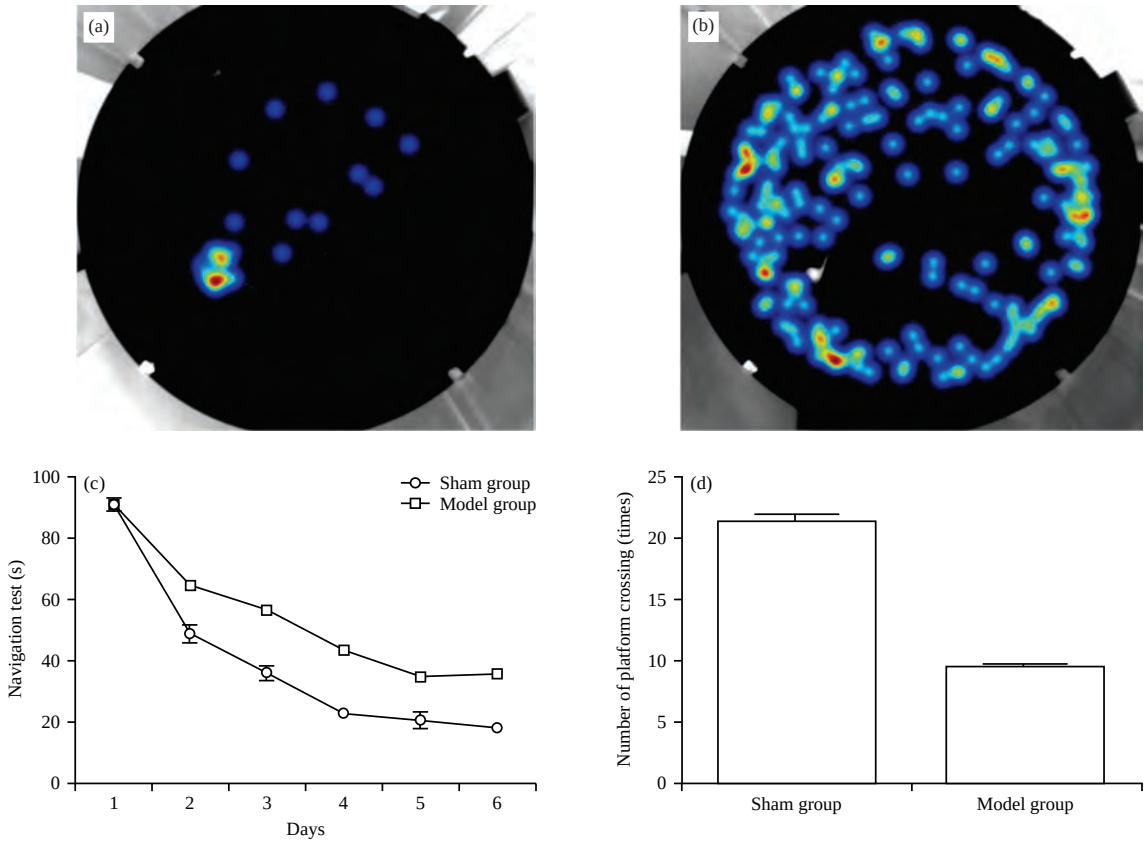

Fig. 1(a-d): Positioning navigation and space exploration in two groups of rats, (a) Positioning navigation heat map of rats in SO group, (b) Positioning navigation heat map of rats in the model group, (c) Time changes of water maze positioning navigation and (d) Number of crossing platforms

significantly decreased ($p<0.01$). Compared with the MC group, the escape latency was significantly decreased ($p<0.01$) and the number of traversing platforms of the HD, MD and LD groups was significantly increased ($p<0.01$), especially in the HD group.

The results of an open field test of rats in each group are shown in Fig. 5. The number of body uprightness and the number of facial washing movements in the open field test of rats in Fig. 5a were counted. The open-field test heat map of rats in the SO group in Fig. 5b, MC group in Fig. 5c, HD group in Fig. 5d, MD group in Fig. 5e and LD group in Fig. 5f were measured. Figure 5a shows the results of the space exploration experiment of rats in each group and the x-axis is the two parameters observed in the space exploration experiment including the number of upright and the number of face washing. The y-axis is the number of times the rats in each group stood upright and face washing. The results of the open-field test showed that compared with the SO group, the number of erection and face washing movements in the darkroom of rats in MC, HD, MD and LD groups was significantly decreased ($p<0.05$). Compared with the MC group, the number of erection and face washing movements in the darkroom of rats in HD, MD and LD groups was significantly increased ($p<0.05$), especially in the HD group (Fig. 5).

Aβ deposition in hippocampal tissue: The expression results of $A\beta^{1-42}$ in brain tissue of rats in each group shown in Fig. 6. The relative expression level of $A\beta^{1-42}$ protein in brain tissue of rats in each group in Fig. 6a was counted and the protein bands of $A\beta^{1-42}$ protein in brain tissue of rats in each group in Fig. 6b were measured. Figure 6a shows the expression level of $A\beta^{1-42}$ in the hippocampus of rats in each group. The x-axis represents the group and the y-axis represents the ratio of the gray value of the $A\beta^{1-42}$ electrophoresis band to the β-actin electrophoresis band. Compared with the SO group, the deposition of $A\beta^{1-42}$ in the hippocampus of rats in MC, HD, MD and LD groups were significantly increased ($p<0.01$). Compared with the MC group, the deposition of $A\beta^{1-42}$ in the hippocampus of rats in HD, MD and LD groups was significantly decreased ($p<0.01$), especially in the HD group.

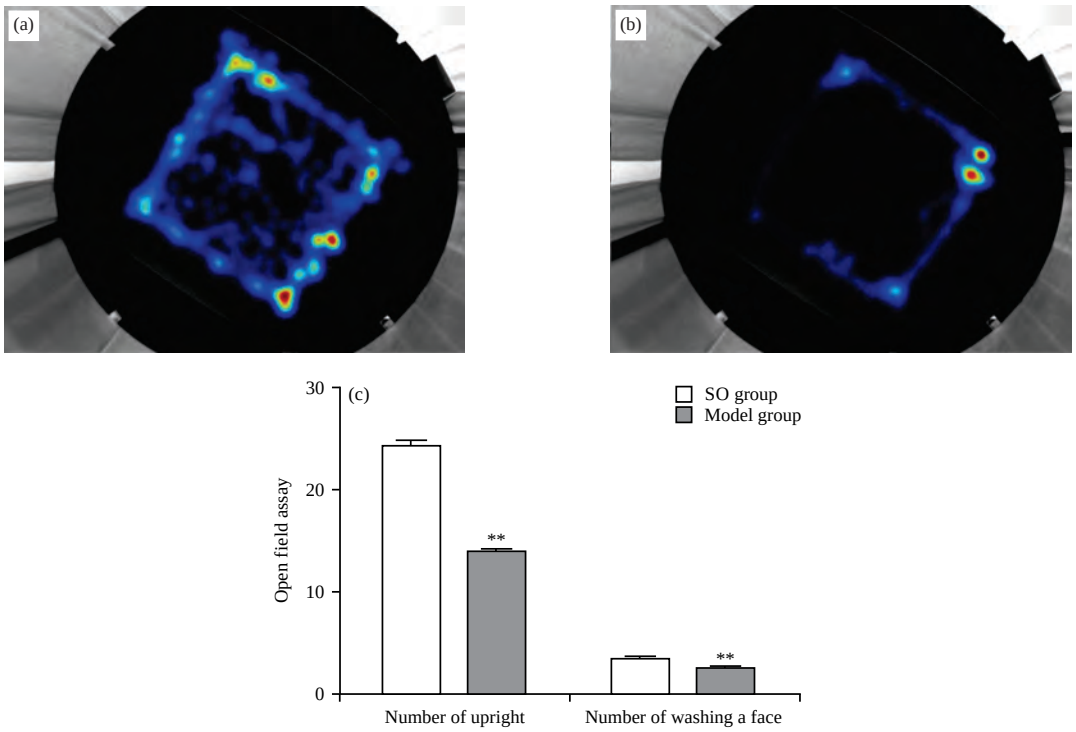

Fig. 2(a-c): Open-field test results of two groups of rats, (a) Open-field test heat map of rats in SO group, (b) Open-field test heat map of rats in model group and (c) Number of body uprightness and the number of facial washing movements in the open field test of rats

**p<0.01 vs. SO group

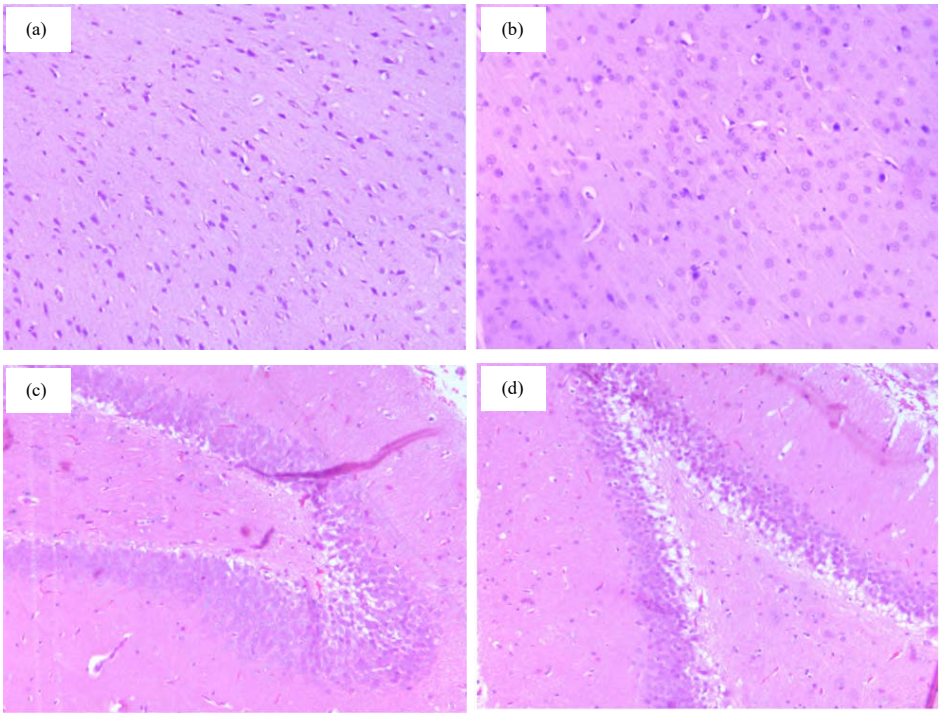

Fig. 3(a-d): Pathology of brain tissue of two groups of rats, (a) Cortex of rat in SO group, (b) Cortex of rat in the model group, (c) Hippocampus of rats in SO group and (d) Hippocampus of rats in the model group

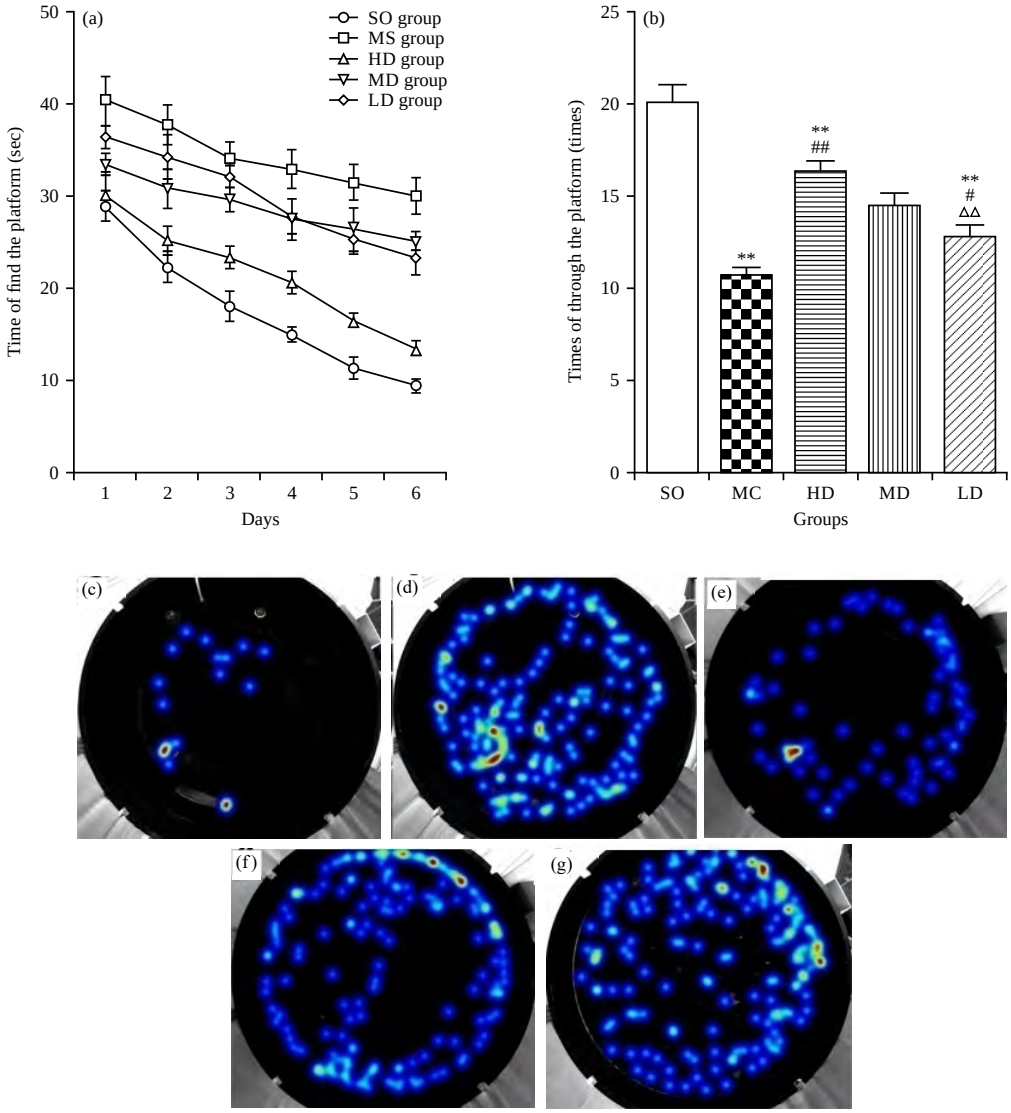

Fig. 4(a-f): Histogram of cognitive function test results for rats in each group, (a) Time changes of water maze positioning navigation, (b) Number of crossing platforms (c) Positioning navigation heat map of rats in SO group, (d) Positioning navigation heat map of rats in MC group, (e) Positioning navigation heat map of rats in HD group, (f) Positioning navigation heat map of rats in MD group and (g) Positioning navigation heat map of rats in LD group

**p<0.01 vs. SO group, #p<0.05 vs. MC group, ##p<0.01 vs. MC group

Inflammatory factor levels in serum and brain tissues: The contents of TNF-α, IL-1β, IL-6 and IFN-γ in serum of rats in the SO group were 36.52±6.32, 35.55±3.88, 19.05±2.36 and 37.61±5.45 pg mL^{-1}, respectively. The contents of TNF-α, IL-1β, IL-6 and IFN-γ in serum of rats in the MC group were 106.23±14.14, 98.68±14.42, 50.29±6.74 and 96.86±11.37 pg mL^{-1}, respectively, which were significantly higher than those in the SO group (p<0.01). The contents of TNF-α, IL-1β, IL-6 and IFN-γ in serum of rats in the HD group were 53.3±6.15, 54.27±5.86, 26.5±2.88 and 57.86±6.69 pg mL^{-1}, respectively, which were significantly higher than those in the SO group and lower than those in the MC group (p<0.01). The contents of TNF-α, IL-1β, IL-6 and IFN-γ in serum of rats in the MD group were 61.71±6.99, 64.78±7.14, 31.27±3.97 and 64.77±7.7 pg mL^{-1}, respectively, which were significantly higher than those in the SO and HD group and lower than those in the MC group (p<0.01). The contents of TNF-α, IL-1β, IL-6 and IFN-γ in serum of rats in LD group were 72.36±9.27, 72.52±6.43, 34.81±4.24 and 69.31±4.89 pg mL^{-1}, respectively, which were significantly higher than those in SO and HD group and lower than those in MC group (p<0.01) in Table 1.

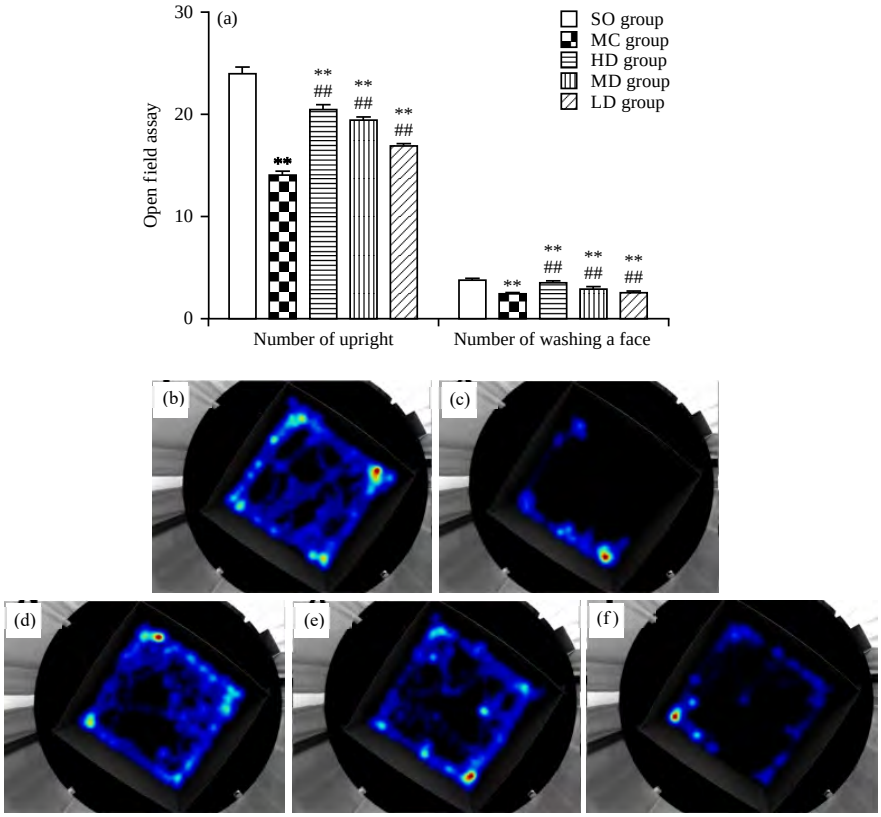

Fig. 5(a-f): Expression of Aβ1-42 in brain tissues of rats in each group, (a) Number of body uprightness and the number of facial washing movements in the open field test of rats, (b) Open-field test heat map of rats in SO group, (c) Open-field test heat map of rats in MC group, (d) Open-field test heat map of rats in HD group, (e) Open-field test heat map of rats in MD group and (f) Open-field test heat map of rats in LD group

**p<0.01 vs. SO group, ##p<0.01 vs. MC group

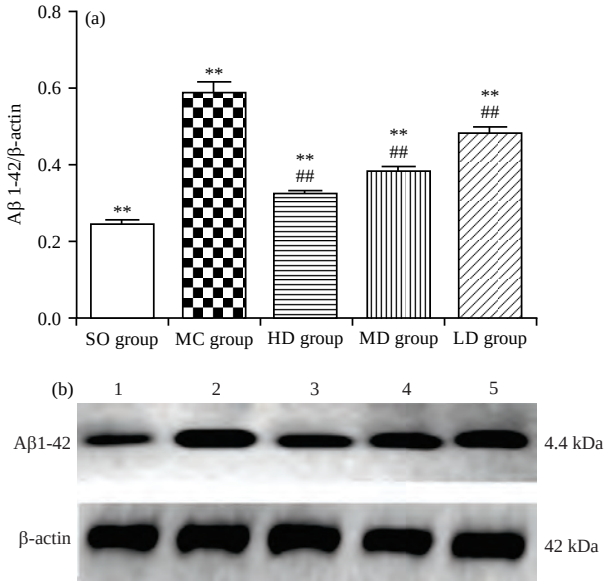

Fig. 6(a-b): Expression of $A\beta^{1-42}$ in the brain tissue of rats, (a) Relative expression level of $A\beta^{1-42}$ protein in brain tissue of rats in each group and (b) Protein bands of $A\beta^{1-42}$ protein in brain tissue of rats in each group

**p<0.01 vs. SO group, ##p<0.01 vs. MC group

Table 1: Content of TNF-α, IL-1β, IL-6 and IFN-γ in serum in each group (pg mL^{-1})

Groups	n	TNF-α	IL-1β	IL-6	IFN-γ
SO	10	36.52±6.32	35.55±3.88	19.05±2.36	37.61±5.45
MC	10	106.23±14.14**	98.68±14.42**	50.29±6.74**	96.86±11.37**
HD	10	53.3±6.15**##	54.27±5.86**##	26.5±2.88**##	57.86±6.69**##
MD	10	61.71±6.99**##△	64.78±7.14**##△△	31.27±3.97**##△	64.77±7.7**##△
LD	10	72.36±9.27**##△△☆	72.52±6.43**##△△☆	34.81±4.24**##△△	69.31±4.89**##△△

*p<0.05, **p<0.01 vs. SO group, #p<0.05, ##p<0.01 vs. MC group, △p<0.05, △△p<0.01 vs. HD group, ☆p<0.05 and ☆☆p<0.01 vs. MD group

Table 2: Content of TNF-α, IL-1β, IL-6 and IFN-γ in brain tissues in each group (pg g^{-1})

Groups	n	TNF-α	IL-1β	IL-6	IFN-γ
SO	6	71.36±2.47	81.1±2.93	49.34±1.28	80.86±1.48
MC	6	100.41±6.89**	115.09±4.53**	61.17±2.48**	112.61±5.63**
HD	6	81.88±4.49**##	90.07±3.08**##	53.42±1.35**##	89.3±3.4**##
MD	6	87.96±4.72**##△	100.48±4.09**##△△	55.41±1.54**##	96.14±3.97**##△△
LD	6	90.96±3.77**##△△	99.92±4.65**##△△	57.61±1.75**##△△☆	98.52±2.97**##△△

*p<0.05, **p<0.01 vs. SO group, #p<0.05, ##p<0.01 vs. MC group, △p<0.05, △△p<0.01 vs. HD group, ☆p<0.05 and ☆☆p 0.01 vs. MD group

Table 3: Microglial marker expression in the brain of rats in each group (number/field of view)

Groups	n	Iba-1/CD80(B7-1)	Iba-1/CD86(B7-2)	Iba-1/CD206	Iba-1/Arg-1
SO	6	2.17±1.17	2.33±1.03	2.33±0.82	2.17±0.75
MC	6	17.17±2.48**	15.17±1.94**	6±1.41**	6.67±1.21**
HD	6	7.5±1.87**##	8.33±1.03**##	13.17±1.47**##	17.33±2.25**##
MD	6	10±1.79**##△	11.5±1.38**##△△	11.5±1.87**##	12±0.89**##△△
LD	6	13.67±2.25**##△△☆☆	13.33±1.63**#△△☆	9.67±1.63**##△△☆	8.5±1.05**##△△☆☆

*p<0.05, **p<0.01 vs. SO group, #p<0.05, ##p<0.01 vs. MC group, △p<0.05, △△p<0.01 vs. HD group, ☆p<0.05 and ☆☆p<0.01 vs. MD group

The contents of TNF-α, IL-1β, IL-6 and IFN-γ in brain tissue of rats in the SO group were 71.36±2.47, 81.1±2.93, 49.34±1.28 and 80.86±1.48 pg g^{-1}, respectively. The contents of TNF-α, IL-1β, IL-6 and IFN-γ in brain tissue of rats in the MC group were 100.41±6.89, 115.09±4.53, 61.17±2.48 and 112.61±5.63 pg g^{-1}, respectively, which was significantly higher than that in the SO group ($p<0.01$). The contents of TNF-α, IL-1β, IL-6 and IFN-γ in brain tissue of rats in the HD group were 81.88±4.49, 90.07±3.08, 53.42±1.35 and 89.3±3.4 pg g^{-1}, respectively, which were significantly higher than those in the SO group and lower than those in the MC group ($p<0.01$). The contents of TNF-α, IL-1β, IL-6 and IFN-γ in brain tissue of rats in the MD group were 87.96±4.72, 100.48±4.09, 55.41±1.54 and 96.14±3.97 pg g^{-1}, respectively, which were significantly higher than those in the SO and HD group and lower than those in MC group ($p<0.01$). The contents of TNF-α, IL-1β, IL-6 and IFN-γ in brain tissue of rats in the LD group were 90.96±3.77, 99.92±4.65, 57.61±1.75 and 98.52±2.97 pg g^{-1}, respectively, which were significantly higher than those in the SO and HD group and lower than those in MC group ($p<0.01$) in Table 2.

Levels of microglia activation and polarization: The expression results of microglia markers in brain tissue of rats in each group are shown in Fig. 7. Figure 7 shows the co-expression level of marker proteins for microglia activation, in which the x-axis represents the double-positive expression of Iba-1/CD80 (B7-1), Iba-1/CD86 (B7-2), Iba-1/cd206 and Iba-1/Arg-1 in each group and the y-axis represents the number of cells with double-positive expression of the above proteins in each visual field. Compared with the SO group, the expression of microglia surface markers in MC, HD, MD and LD groups showed that Iba-1/CD80 (B7-1) (Fig. S1), Iba-1/CD86 (B7-2) (Fig. S2) and Iba-1/CD206 (Fig. S3), Iba-1/Arg-1 (Fig. S4) double-positive cells were significantly increased in Table 3 ($p<0.01$). Compared with the MC group, the number of Iba-1/CD80 (B7-1) and Iba-1/CD86 (B7-2) double-positive cells was significantly decreased ($p<0.01$), but the number of Iba-1/CD206 and Iba-1/Arg-1 double-positive cells was significantly increased ($p<0.01$) in HD, MD and LD groups.

Activation level of TLR4/MYD88/NF-κB signalling pathway in the cerebral cortex: The TLR4, MyD88 and NF in brain tissue of rats in each group NF-κB p-NF-κB the expression of the protein is shown in Fig. 8. The relative expression levels of TLR4, MYD88, NF-κB and p-NF-κB protein in brain tissue of rats in each group in Fig. 8a was counted and the protein bands of TLR4, MYD88, NF-κB and p-NF-κB protein in brain tissue of rats in each group in Fig. 8b were measured. Figure 8a shows the expression level of TLR4, MyD88 and NF-κB and p-NF-κB in brain tissue of rats in each group. The x-axis represents the expression level of TLR4, MyD88 and NF-κB and p-NF-κB and the y-axis represents the ratio of the gray value of the above-target protein electrophoresis band to β-actin electrophoresis band. The expression levels of TLR4, MYD88, NF-κB and p-NF-κB in the cerebral cortex of rats in MC, HD, MD and LD groups were significantly higher than those in the SO

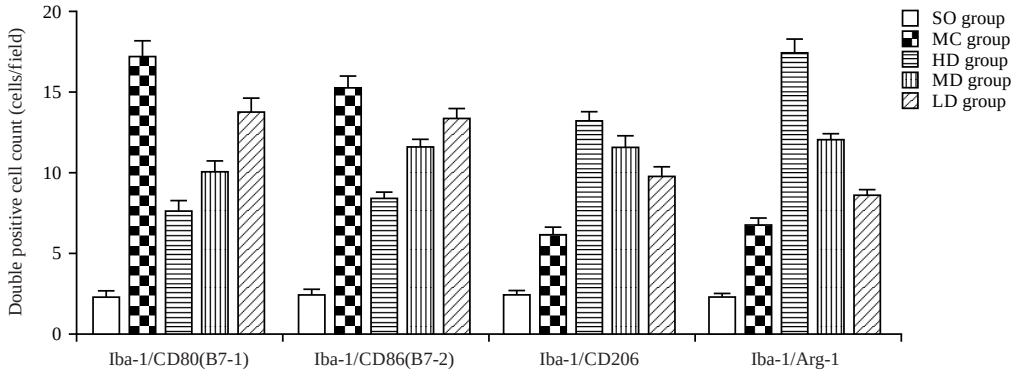

Fig. 7: Histogram of microglia marker expression in the brain of each group of rats

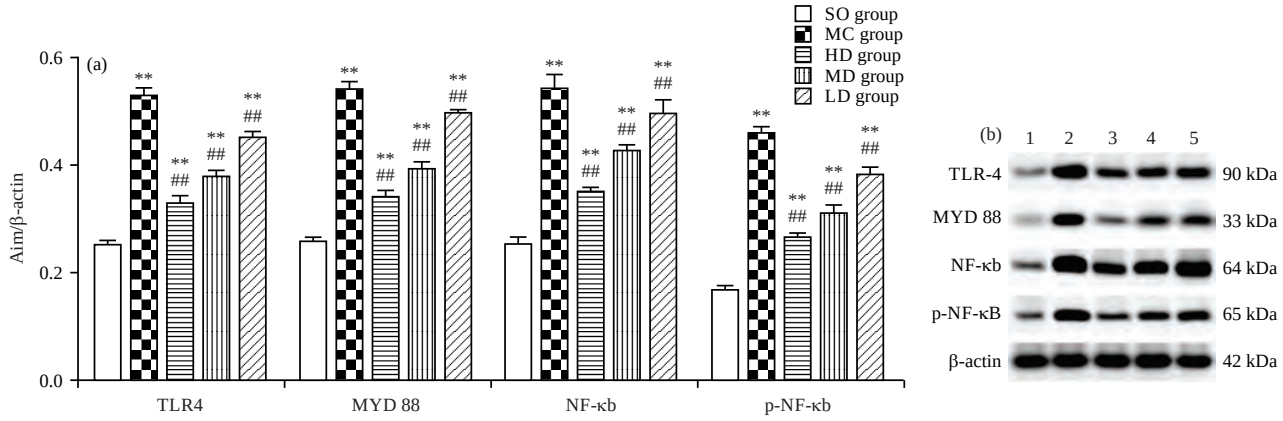

Fig. 8(a-b): Expression of TLR4, MYD88, NF-κB and p-NF-κB protein in the brain of rats, (a) Relative expression levels of TLR4, MYD88, NF-κB and p-NF-κB protein in brain tissue of rats in each group and (b) Protein bands of TLR4, MYD88, NF-κB and p-NF-κB protein in brain tissue of rats in each group

**p<0.01 vs. SO group, ##p<0.01 vs. MC group

group (Fig. S5) (p<0.01). Compared with the MC group, the expression levels of TLR4, MYD88, NF-κB and p-NF-κB in the brain tissue of the rats in HD, MD and LD groups were significantly decreased (p<0.01).

DISCUSSION

Microglia, originating from monocytes in the bone marrow with a high degree of plasticity and very similar biological properties to macrophages, is intrinsic immune cells in the central nervous system. The results showed that microglia was involved in the development of various neurodegenerative diseases[12]. Microglia exert effects through housekeeping functions such as chemotaxis and phagocytosis to stabilize the body's steady state, whereas abnormal housekeeping functions often induces the development of neurodegenerative diseases[13]. It has been reported that the onset of AD is closely related to the lack of beta-amyloid clearance, which in turn allows microglia to exert neurotoxicity and promote the progression of neurodegenerative disease and that persistently activated microglia aggravate the neuronal lesions of neurodegenerative disease[14,15]. The transition of microglia from M0-resting to M1-activated states is a key factor in mediating the development of an inflammatory response to AD[16,17]. Therefore, elucidation of the mechanism of microglial transition from M0 to M1-activation and M2-polarization states may be a key step in elucidating the development of AD.

Kaixin San is from the ancient book *Qianjin Fang*. The formula contains ginseng, polygala, tuckahoe and rhizome acorigraminei. It is now used in the treatment of diseases such as Alzheimer's disease and vascular dementia with memory dysfunction as the main manifestation[7-9]. Ginsenoside Rb2, a major component of the prescription, has been reported to reduce damage to rat cortical neurons and protect them from microglial activation[11]. It can be seen that the regulation of microglial activation by KS may be the main mechanism of its treatment for Alzheimer's disease.

The experimental results of the water maze and open-field showed that the cognitive function of the rats in the model group was abnormal. During 5 days of training, the positioning time of the rats in the SO group was shortened day by day and decreased rapidly, which indicated that the rats in this group had good memory for platform position, while the positioning time of rats in the model group was shortened gradually, but the change was not obvious. On the 6th day, when the space exploration experiment was carried out, the number of passing through the quadrant of the platform was significantly higher than that of the model group, indicating that the memory function of the model group rats was impaired. In addition, the open-field test showed that the rats in the model group were much slower than those in the SO group in exploring the strange environment. The results of brain histopathology showed that the damage of neurons was obvious in the model group. Based on the results of the evaluation of the model, we believe that the injection of $A\beta^{1-42}$ into the lateral ventricle can replicate the AD rat model stably. The model copying method of this study provides an important guarantee for the accuracy of our subsequent studies.

After 6 weeks of treatment, the results of the cognitive function test in each group suggested that the cognitive function of the rats in the HD, MD and LD group was improved and that in the HD group was the most obvious, indicating that the effect of JKS on cognitive function in AD rats was reliable. At the same time, the results of Aβ deposition in the hippocampus of rats in each group showed that JKS could significantly reduce the deposition of Aβ in the hippocampus of AD rats in a dose-dependent manner and that in the HD group was the most obvious. This result further confirms the results of our team's clinical observations regarding the use of JKS in the treatment of AD patients.

Chronic inflammation has been reported almost throughout the onset of AD[18,19] and anti-inflammatory therapy is one of the important treatment methods for AD. To determine the anti-inflammatory effect of JKS on AD, the contents of TNF-α, IL-1β, IL-6 and IFN-γ in brain tissue and serum of rats were measured. The results showed that the levels of TNF-α, IL-1β, IL-6 and IFN-γ in brain tissue and serum of rats in the MC group were significantly higher. The levels of TNF-α, IL-1β, IL-6 and IFN-γ in brain tissue of rats in HD, MD and LD groups were significantly lower than those in the MC group in a dose-dependent manner. These results suggested that JKS has a good anti-inflammatory effect, which may be one of the reasons why JKS can improve the cognitive function of AD rats.

Microglia are intrinsic immune cells in the central nervous system and are involved in the development of inflammatory responses in brain tissue. When microglia are converted from M0-resting status to M1 type, activated microglia are involved in the development of inflammatory responses in the brain. When M0 type microglia are polarized to M2 type, they play an anti-inflammatory role[20]. Therefore, we observed the activation and polarization effects of JKS on microglia by detecting the expression of microglial markers in the brain of each group of rats. The Iba-1 was the specific expression molecule on the surface of microglia. The surface of M1 microglia mainly expressed CD80 (B7-1) and CD86 (B7-2). In addition to expressing Iba-1, the surface of M2 microglia also expressed CD206 and Arg-1. The results showed that the double-positive expression of Iba-1/CD80 (B7-1), Iba-1/CD86 (B7-2), Iba-1/CD206 and Iba-1/Arg-1 in the brain of the model group were significantly increased. The results suggested that the activation and polarization of microglia were induced by $A\beta^{1-42}$. On the one hand, excessive deposition of Aβ activated the microglia to M1 type, which mediated the occurrence of inflammatory reaction. On the other hand, the self-protection of the body under emergency conditions is initiated and the anti-inflammatory effect is exerted by polarizing the microglia to M2 type to protect the neurons from the inflammatory response. After the intervention, the number of Iba-1/CD80 (B7-1) and Iba-1/CD86 (B7-2) double-positive cells in the brain tissue of AD rats was significantly decreased, while the number of Iba-1/CD206 and Iba-1/Arg-1 double-positive cells was significantly increased. The JKS changed the distribution of microglia subtypes in the brain of AD rats, reduced the proportion of M1 microglia, increased the proportion of M2 microglia and then played an anti-inflammatory role.

The TLR4/MYD88/NF-κB signalling pathway is one of the important pathways that mediate the inflammatory response. Numerous reports have shown that the phenotypic transformation of microglia is closely related to the activation of this signalling pathway[21]. Therefore, we further examined the activation level of the TLR4/MyD88/NF-κB signalling pathway to elucidate the regulatory mechanism of JKS on the phenotypic transformation of microglia. The results showed that the expression levels of TLR4, MyD88, NF-κB and p-NF-κB in the brain of AD rats significantly increased. The JKS inhibited the expression levels of TLR4, MyD88, NF-κB and p-NF-κB in the brain of AD rats in a dose-dependent manner, especially in the HD group. These results suggested that JKS has significant inhibitory effects on the abnormal activated TLR4/MyD88/NF-κB signalling pathway in AD rats, which is closely related to its inhibitory effect on the activation of microglia from M0 type to M1 type and promoting the polarization of microglia from M0 type to M2 type.

CONCLUSION

Jia Wei Kai Xin San could reduce the deposition of Aβ in the brain tissue of AD rats, inhibit the expression of

inflammatory factors and the activation of microglia to M1 type, promote the polarization of microglia to M2 type, inhibit the abnormal activation of TLR4/MYD88/NF-κB signalling pathway to improve the cognitive function of AD rats.

SIGNIFICANCE STATEMENT

This study explored that Jia Wei Kai Xin San could improve cognitive function by inhibiting the activation of microglia which will provide a new treatment idea in the field of treating Alzheimer's disease with Traditional Chinese Medicine. At the same time, the mechanism of this therapeutic effect was preliminarily discussed which laid a solid foundation for further research.

REFERENCES

1. Beckman, D., S. Ott, K. Donis-Cox, W.G. Janssen and E. Bliss-Moreau *et al*., 2019. Oligomeric Aβ in the monkey brain impacts synaptic integrity and induces accelerated cortical aging. PNAS, 116: 26239-26246.
2. Graham, W.V., A. Bonito-Oliva and T.P. Sakmar, 2017. Update on Alzheimer's disease therapy and prevention strategies. Annu. Rev. Med., 68: 413-430.
3. Heckmann, B.L., B.J.W. Teubner, B. Tummers, E. Boada-Romero and L. Harris *et al*., 2019. LC3-associated endocytosis facilitates β-amyloid clearance and mitigates neurodegeneration in murine Alzheimer's disease. Cell, 178: 536-551.e14.
4. Almolda, B., C. de Labra, I. Barrera, A. Gruart and J.M. Delgado-Garcia *et al*., 2015. Alterations in microglial phenotype and hippocampal neuronal function in transgenic mice with astrocyte-targeted production of interleukin-10. Brain, Behav., Immun., 45: 80-97.
5. Chiarini, A., I.D. Pra, J.F. Whitfield and U. Armato, 2006. The killing of neurons by beta-amyloid peptides, prions, and pro-inflammatory cytokines. Ital. J. Anat. Embryol., 111: 221-246.
6. Li, X.H., Y.Y. Deng, F. Li, J.S. Shi and Q.H. Gong, 2016. Neuroprotective effects of sodium hydrosulfide against β-amyloid-induced neurotoxicity. Int. J. Mol. Med., 38: 1152-1160.
7. Li, M.H., J. Zhang, R.Q. Zhao, X.Z. Dong and Y.Hu *et al*., 2016. Effect of six class of Kaixin San formulas on pharmacological and preliminary mechanism of Alzheimer's disease mice. Zhongguo Zhong Yao Za Zhi, 41: 1269-1274.
8. Zhang, B., Y. Li, J.W. Liu, X.W. Liu, W. Wen, Y. Cui and S.M. Huang, 2018. Postsynaptic GluR2 involved in amelioration of Aβ-induced memory dysfunction by KAIXIN-San through rescuing hippocampal LTP in mice. Rejuvenation Res., 22: 131-137.
9. Li, X., W. Wen, P. Li, Y. Fu and H. Chen *et al*., 2021. Mitochondrial protection and against glutamate neurotoxicity via Shh/Ptch1 signaling pathway to ameliorate cognitive dysfunction by Kaixin San in multi-infarct dementia rats. Oxid. Med. Cell. Longevity, Vol. 2021. 10.1155/2021/5590745.
10. Wang, H.X., N. Jiang, J.W. Lv, S.S. Liu and X.M. Liu, 2020. Review of anti-depression and improving learning and memory activities of kaixin powder and their mechanisms. Chin. Tradit. Herb. Drugs., 51: 3802-3813.
11. Wu, C.F., X.L. Bi, J.Y. Yang, J.Y. Zhan and Y.X. Dong *et al*., 2007. Differential effects of ginsenosides on NO and TNF-α production by LPS-activated N9 microglia. Int. Immunopharmacol., 7: 313-320.
12. Subhramanyam, C.S., C. Wang, Q. Hu and S.T. Dheen, 2019. Microglia-mediated neuroinflammation in neurodegenerative diseases. Semin. Cell Dev. Biol., 94: 112-120.
13. Hickman, S., S. Izzy, P. Sen, L. Morsett and J.E. Khoury, 2018. Microglia in neurodegeneration. Nat. Neurosci., 21: 1359-1369.
14. Ge, X., D.M. Zhang, M.M. Li, Y. Zhang and X.Y. Zhu *et al*., 2019. Microglial LOX-1/MAPKs/NF-κB positive loop promotes the vicious cycle of neuroinflammation and neural injury. Int. Immunopharmacol., 70: 187-200.
15. Liddelow, S.A., K.A. Guttenplan, L.E. Clarke, F.C. Bennett and C.J. Bohlen *et al*., 2017. Neurotoxic reactive astrocytes are induced by activated microglia. Nature, 541: 481-487.
16. Hansen, D.V., J.E. Hanson and M. Sheng, 2017. Microglia in Alzheimer's disease. J. Cell Biol., 217: 459-472.
17. Rentzos, M., G.P. Paraskevas, E. Kapaki, C. Nikolaou and M. Zoga *et al*., 2006. Interleukin-12 is reduced in cerebrospinal fluid of patients with Alzheimer's disease and frontotemporal dementia. J. Neurol. Sci., 249: 110-114.
18. Kim, S.M., J. Song, S. Kim, C. Han and M.H. Park *et al*., 2011. Identification of peripheral inflammatory markers between normal control and Alzheimer's disease. BMC Neurol., Vol. 11. 10.1186/1471-2377-11-51.
19. Zhang, Y., Y. Zhao, J. Zhang, Y. Gao and S. Li *et al*., 2021. Ginkgolide b inhibits NLRP3 inflammasome activation and promotes microglial M2 polarization in $A\beta_{1-42}$-induced microglia cells. Neurosci. Lett., Vol. 764. 10.1016/j.neulet.2021.136206.
20. Xu, X.J., J.B. Long, K.Y. Jin, L.B. Chen, X.Y. Lu and X.H. Fan, 2021. Danshen-chuanxiongqin injection attenuates cerebral ischemic stroke by inhibiting neuroinflammation via the TLR2/TLR4-MyD88-NF-κB pathway in tMCAO mice. Chin. J. Nat. Med., 19: 772-783.
21. Zhao, Z., F. Li, J. Ning, R. Peng and J. Shang *et al*.,2021. Novel compound FLZ alleviates rotenone-induced pd mouse model by suppressing TLR4/MyD88/NF-κB pathway through microbiota–gut–brain axis. Acta Pharmaceutica Sinica B, 11: 2859-2879.

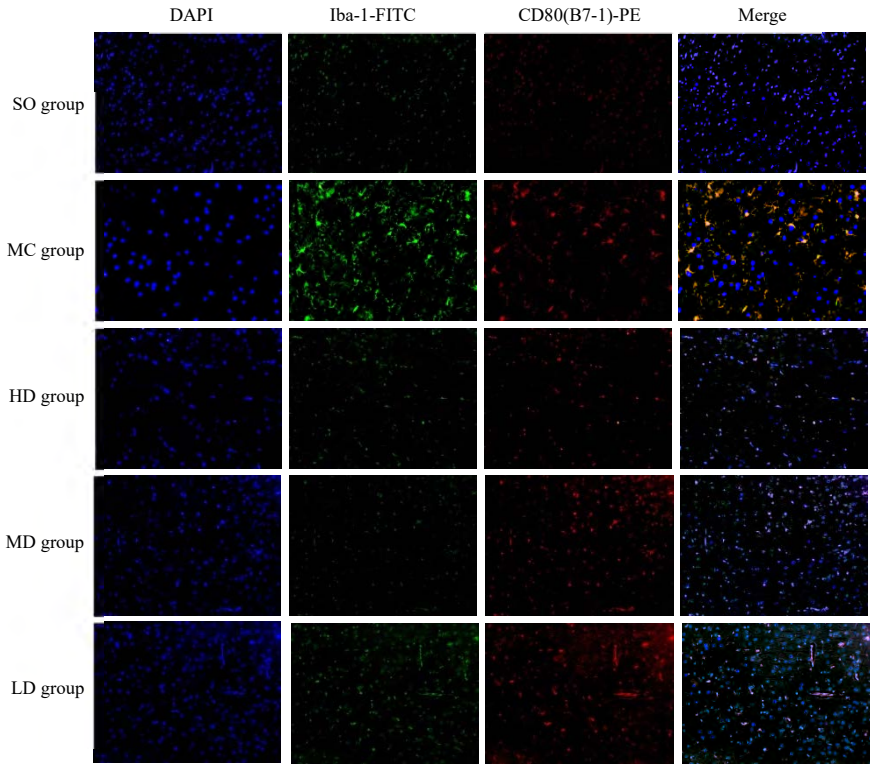

Fig. S1: Immunofluorescence images of Iba-1/CD80 (B7-1) co-expression in rat brain tissue

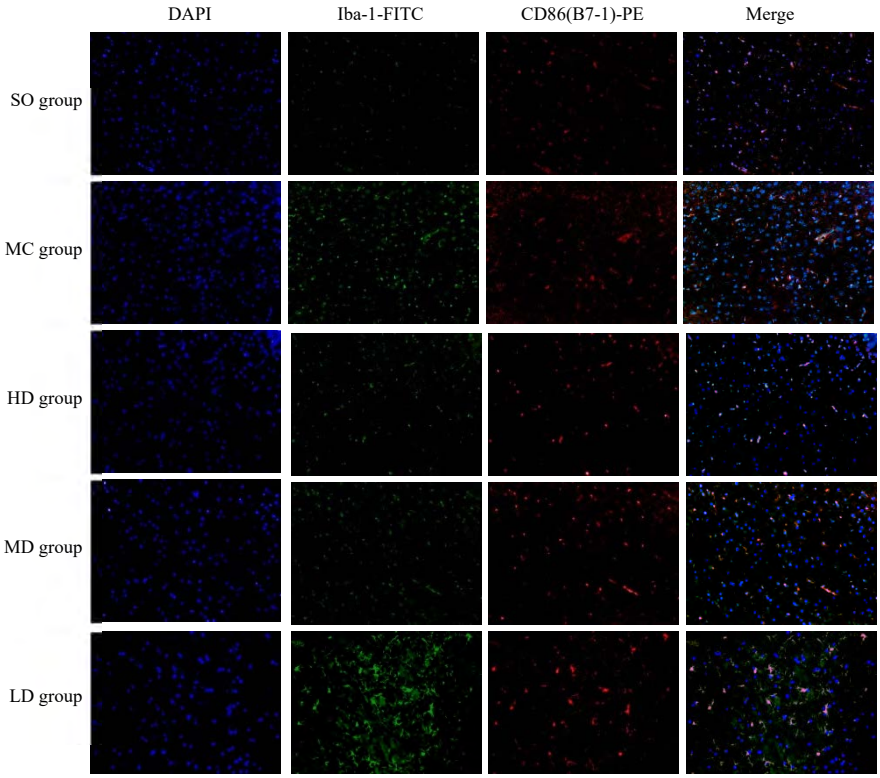

Fig. S2: Immunofluorescence images of Iba-1/CD86 (B7-2) co-expression in rat brain tissue

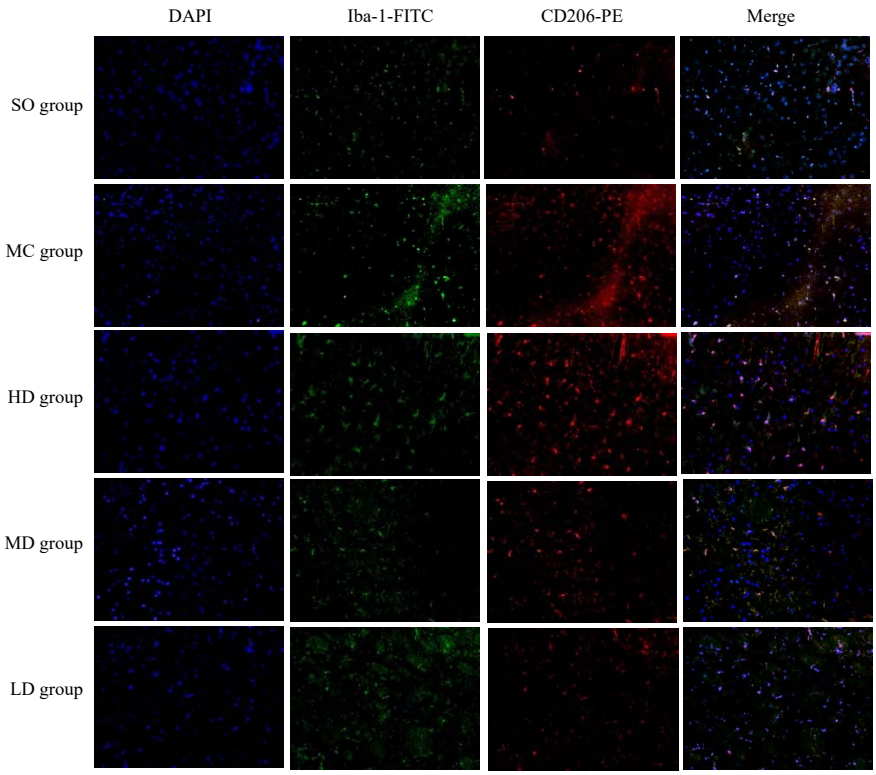

Fig. S3: Immunofluorescence photographs of the co-expression of Iba-1/CD206 in the brain of each group of rats

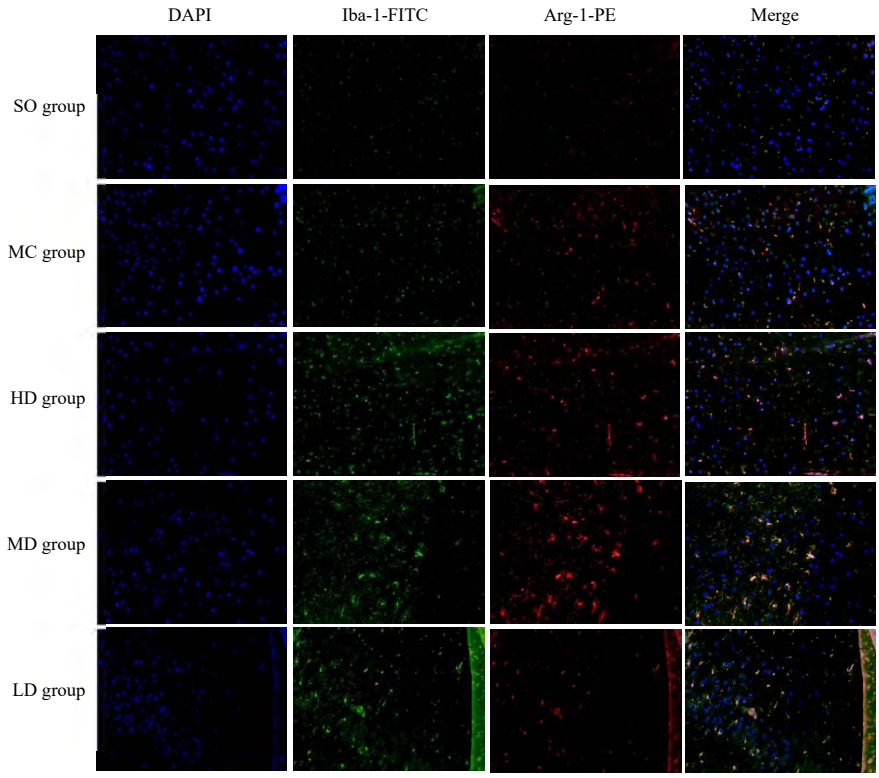

Fig. S4: Immunofluorescence images of Iba-1/Arg-1 co-expression in rat brain tissues of each group

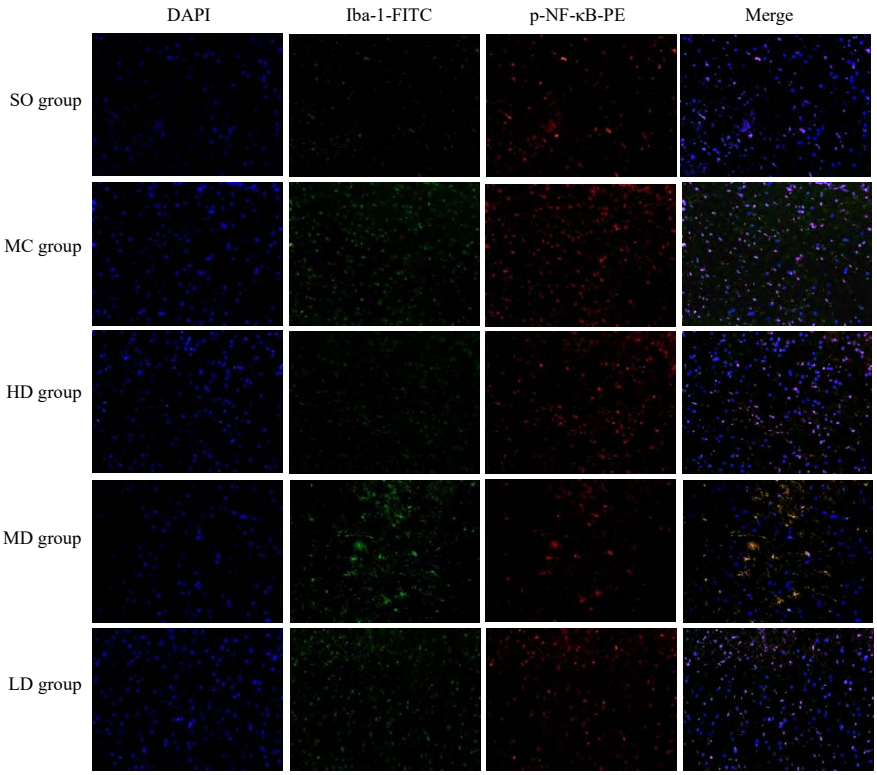

Fig. S5: Immunofluorescence images of Iba-1/p-NF-κB co-expression in rat brain tissue